Journal of the Indian Society of Remote Sensing (December 2019) 47(12):2113–2127
https://doi.org/10.1007/s12524-019-01040-3

RESEARCH ARTICLE

Image Fusion of SAR and Optical Images for Identifying Antarctic Ice Features

Esha Shah[1] · P. Jayaprasad[2] · M. E. James[1]

Received: 4 January 2019 / Accepted: 23 August 2019 / Published online: 15 October 2019

Abstract
Remote sensing data plays an important role in extracting thematic information from various sensors having different spectral, spatial and temporal resolutions. The present study aims at fusion of Radar Imaging Satellite-1 Fine Resolution Stripmap-1 and ResourceSAT-2 Linear Imaging Self Scanning Scanner-4 (LISS-4) images over Indian Antarctic Research Station Maitri and its surroundings to generate a better product which contains the characteristics of both the spectral information from LISS-4 and the spatial details of SAR. Different pixel-based fusion techniques such as Brovey Transform, Principal Component Analysis (PCA), Intensity Hue Saturation and Wavelet Principal Component Analysis (W-PCA) have been used in the present study. These image fusion techniques have been applied for the whole scene as well as for individual surface features like melt ponds, crevasses, freshwater lake, blue ice, oasis and lake ice for better discrimination of features. Quality assessment is performed by evaluating the performance of these algorithms using visual, spatial (High Pass Correlation Coefficient and Entropy) and spectral (Root Mean Square Error, Correlation Coefficient, ERGAS and Universal Quality Index) parameters. It is found that the identification of certain features such as crevasses, blue ice, melt ponds and lake ice has been improved with fused images compared to the original multi-spectral and SAR images. PCA and W-PCA fusion techniques offer better performance as compared to the rest of the techniques.

Keywords Antarctic ice features · Feature extraction · Image fusion · Image merging · RISAT-1 FRS-1 · SAR · ResourceSAT-2 LISS-4

Introduction

The multi-spectral (MS) sensors operating in optical wavelengths provide information regarding reflective or emissive characteristics of the targets. Since the optical images contain rich details, it is relatively easier to interpret. However, optical images are affected by illumination conditions and atmospheric conditions at the time of capturing the images. This inherent problem of MS sensors is minimized by using Radars which operate with its own source of illumination at microwave frequencies. The Synthetic Aperture Radar (SAR) can generate images during all time as well as all weather conditions. The SAR uses the backscattered power in the antenna direction. The brightness in SAR images depends upon roughness, geometry and material contents of the surface and wavelength of observation. The absorption or scattering of microwave energy depends on the dielectric constant of the surface. The SAR has an added advantage that it can penetrate the surface to a certain extent depending upon the operating frequency and the dielectric constant of the target. In general, SAR images contain useful information that cannot be found in MS images. However, due to limited number of bands as well as the effects caused by speckle noise, slant-range imaging, foreshortening, layover and shadows, the SAR images are relatively difficult to interpret compared to optical images. The SAR images, which

✉ P. Jayaprasad
jayaprasadp@gmail.com

Esha Shah
eshu7456@gmail.com

M. E. James
mejames1962@gmail.com

[1] Department of Physics, Electronics and Space Sciences, Gujarat University, Ahmedabad 380009, India

[2] Space Applications Centre (ISRO), Ahmedabad 380015, India

give better spatial characteristics, are often used as a complementary technique to traditional MS remote sensing which gives better spectral characteristics.

Image fusion technique is defined as the process of combining information from two or more images of a scene into a single composite image that is more informative and more suitable for visual perception (Karhe and Chandratre 2016). It is a technique generally used to combine the spatial information of a high-resolution panchromatic (PAN) image with the spectral information of a low-resolution MS image for the same area to get more information, which is not achieved by using each image alone. So, the fusion of multi-sensor and multi-resolution images is an effective method for exploiting the complimentary nature of different data types for better interpretation.

A number of studies have been carried out on the fusion of PAN images with MS images. Ehlers et al. (2010) carried out a comparative analysis of various fusion techniques for better interpretation of surface features in terms of spectral characteristics preservation as well as spatial improvement. Atta (2012) tested different fusion methods to evaluate their enhancement capabilities to extract different surface features. Jawak and Luis (2013) employed dataset derived from the very high resolution of the WorldView-2 satellite (Panchromatic and MS) for two test sites (one over an urban area and the other over Antarctica), to comprehensively evaluate the performance of PAN-sharpening algorithms.

Many studies used optical MS and microwave SAR images separately, but a few attempts have been made to jointly examine these imageries using fusion techniques for feature extraction (Ramadan et al. 2006; Pal et al. 2007; Rahman et al. 2010). Fusing an optical image having high spectral resolution with a SAR image having high spatial resolution will provide an image with high spatial (sharp edges, texture) as well as high spectral information (object identification) and make it easier to detect interpret various features (Misra et al. 2012). But, it is challenging to match and co-register SAR and optical MS images due to the different geometric and radiometric properties of the two observation type techniques (Schmitt et al. 2017). A good fusion algorithm should not distort the colour content of the original MS image while enhancing its spatial resolution. But, due to the significant differences between the imaging mechanisms of SAR and MS optical images, when SAR and MS images are fused, the differences in grey values between the intensity image and the SAR image become obvious. After the image fusion, this difference causes substantial colour distortion in the fused images.

Ricchetti (2001) developed a technique to fuse an ERS-1 SAR image and a Landsat Thematic Mapper (TM) image to improve the interpretation of lithology boundaries and recognition of structural features. Chibani (2007) described a new method for integrating Panchromatic and SAR features into MS images using the modified Brovey Transform and the Wavelet Decomposition techniques. Erener and Sebnem (2012) analysed earth features such as individual artificial structures and urban settlement using TerraSar-X and high-resolution Quickbird images.

The basic objective of the present study is to demonstrate the potential of image fusion of high spectral resolution ResourceSAT LISS-4 MS image and high spatial resolution RISAT-1 SAR FRS-1 image for better identification of Antarctic ice features such as lake ice, snow, blue ice, crevasses, and melt ponds over the Indian Antarctic research station Maitri and its surroundings. The crevasse detection is very important in Maitri and surroundings as the Indian expedition team has to transport the decanted items from India Bay to Maitri covering a distance of approximately 100 km through convoy operations using Pistenbully and other snow transport vehicles. The second aim of the study is to compare efficiency of various techniques in fusing a high spectral resolution MS image and high spatial resolution SAR image containing various ice features.

Study Area and Data Used

The study area covers the Indian Antarctic research station, Maitri (70°45′53″ S latitude and 11°44′03″ E longitude) located at Schirmacher oasis and its surrounding area on central Queen Maud Land in Antarctica.

In the present study, SAR FRS-1 image from RISAT-1 and LISS-4 optical MS image from ResourceSAT-2 have been fused, using ERDAS IMAGINE software. The LISS-4 is a high-resolution (5.8 m) sensor onboard the ResourceSAT-2 satellite, having three spectral bands such as 0.52–0.59 µm (B2-G), 0.62–0.68 µm (B3-R) and 0.77–0.86 µm (B4-NIR) with 70 km swath. RISAT-1 is a C-band SAR (5.35 GHz), launched on 26 April 2012, having five different modes in which FRS-1 with 2.25 m spatial resolution and 25 km swath is a conventional stripmap mode of SAR operation (Misra et al. 2013). Figure 1 shows the RISAT-1 FRS-1 image acquired on 2 March 2015 and ResourceSAT-2 LISS-4 image 28 Feb 2015 acquired over the study area. This region covers different Antarctic features such as ice shelf, snow, blue ice, oasis, freshwater lake, lake ice, melt ponds, crevasses, and ice dunes.

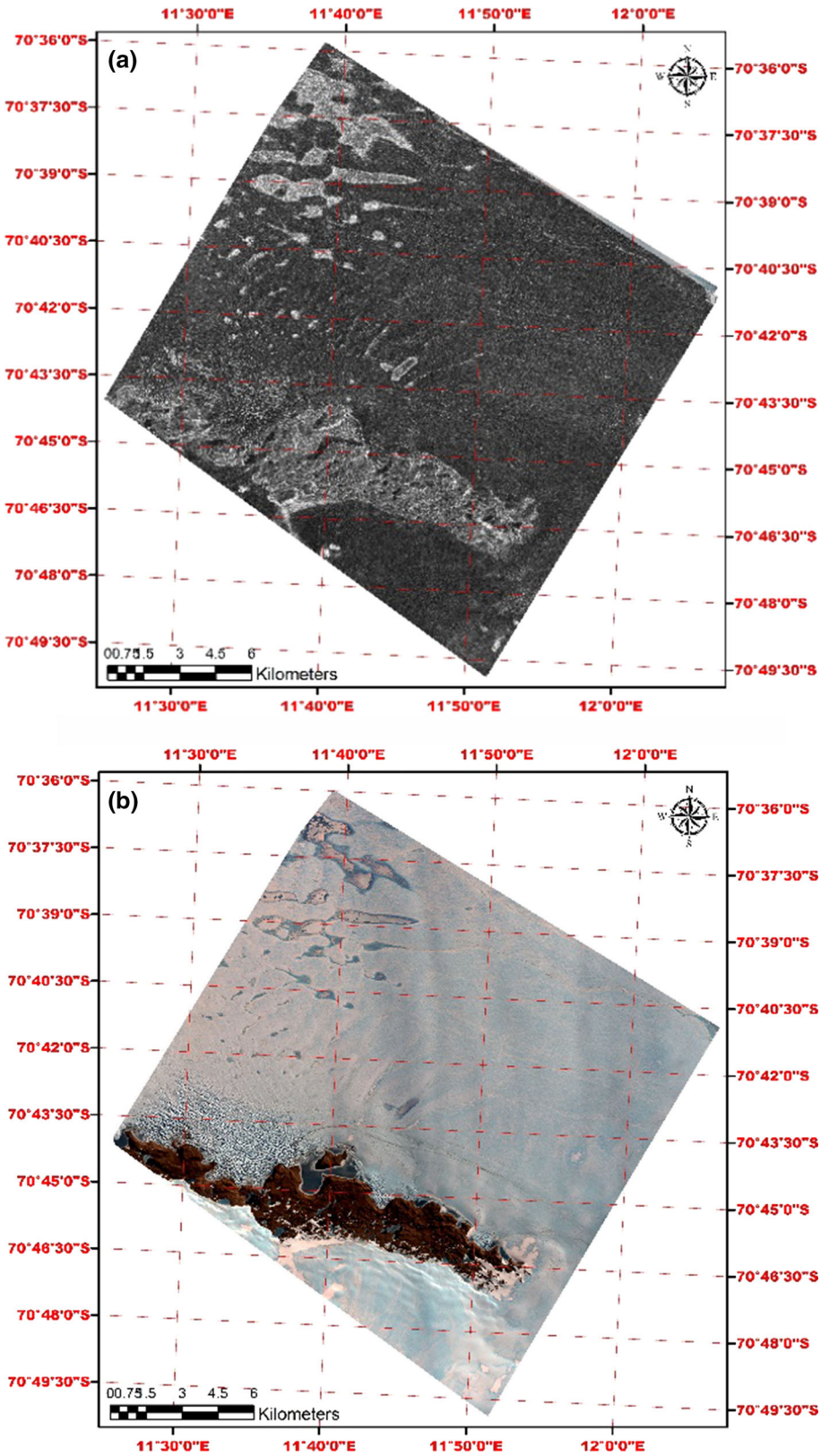

Fig. 1 Images of the study area **a** RISAT-1 FRS-1 SAR (RH polarization), **b** ResourceSAT-2 LISS-4 (B2-B, B3-G, B4-R)

Methodology

RISAT SAR FRS-1 and ResourceSAT-2 LISS-4 images have been procured from National Remote Sensing Centre (NRSC). The FRS-1 scene has been already geo-referenced by SARC module developed at Space Application Centre (ISRO). The overall methodology is discussed in the following sections.

Co-registration of FRS-1 and LISS-4 Images

RISAT FRS-1 SLC product has been converted to ortho-rectified ground range detected (GRD) product using the software module developed by the SAC (ISRO). This output with 2.25 m resolution has been treated as the reference image. The LISS-4 image has been registered with FRS-1 using ERDAS IMAGINE 2015 software. Twenty-one Ground Control Points (GCPs) were selected for the image-to-image co-registration. The Root Mean Square Error (RMSE) achieved between SAR and optical images is slightly higher (4.5 m) because it was difficult to obtain distributed and accurate GCPs as the area is covered mostly by snow. One has to depend on rocky outcrops or lake edges for GCPs because all other features such as snow, melt ponds, and crevasses keep changing within 2 day difference. We have taken maximum care to minimize the error in choosing GCPs.

The SAR images generally may have speckle noises because of the nature of the radar imagery. These speckles affect the quality of the fused products since they are transferred into the fused images by image fusion algorithms. For this reason, SAR images have been de-speckled before image fusion processes. In this study, speckles were smoothed using the algorithm proposed by Lee (1981). Image fusion essentially occurs when the involved images have the same spatial resolution. Thus, the low-resolution MS image has been resampled such that they have the same spatial resolution with the SAR image. For resampling, the nearest neighbour method has been used because other methods may have deteriorating effect on the original structure of the MS. Different techniques have been used for fusion of geo-referenced SAR image with LISS-4 images.

Image Fusion Techniques

There are different methods of fusion such as IHS, M-IHS, Brovey Transformation, Wavelet transforms, PCA, Gram-Schmidt (GS) transformation, HPF (High Pass Frequency), Ehlers method, two-dimensional DWT (Discrete Wavelet Transformation), fusing through stochastic gradient boosting (SGB) regression, and fusing through adaptive boosting (AdaBoost) regression. Though there are many approaches to fusion, there is no superior fusion technique and the best technique should be chosen based on application. In the present study, the four standard techniques have been used for fusion and are discussed below.

Brovey Transform (BT)

The BT uses ratio method for fusing two images. In this method, all bands are used according to the set of equations (Eq. 1) to create a new image (Jain 2007).

$$\begin{aligned} \text{DNB1 new} &= [(\text{DNB1}/\text{DNB1}) + \text{DNB2} + \text{DNB3}] \times [\text{DN SAR}] \\ \text{DNB2 new} &= [(\text{DNB2}/\text{DNB1}) + \text{DNB2} + \text{DNB3}] \times [\text{DN SAR}] \\ \text{DNB3 new} &= [(\text{DNB3}/\text{DNB1}) + \text{DNB2} + \text{DNB3}] \times [\text{DN SAR}] \end{aligned} \tag{1}$$

where B represents the bands.

The BT retains the corresponding spectral feature of each pixel and transforms all the luminance information of the MS image into a high-resolution SAR image (Mandhare et al. 2013). The BT will probably lead to colour distortion especially when the spectral range of the input images are different or when thy have different long-term temporal changes (Gharbia et al. 2014).

Intensity Hue Saturation (IHS)

The IHS is a classical technique to fuse high spatial resolution single band PAN/SAR image with low spatial resolution MS image (Gharbia et al. 2014). The IHS method transforms a low-resolution 3-band RGB image to IHS components, where I refers to the total brightness of the image, H to the dominant or average wavelength of the light contributing to the colour, and S to the purity of the colour. In the IHS space, spectral information is mostly reflected on the hue and the saturation (Al-Wassai et al. 2011a). The intensity component, which represents the spatial information of the image, is replaced with a high-resolution PAN/SAR image to enhance the spatial resolution. By reverse transformation from IHS to RGB, a high spatial resolution MS image is produced. The schematic of IHS transformation is shown in Fig. 2.

The underlying assumption of both BT and IHS is that the PAN image is equivalent to the intensity image obtained from the RGB image. However, this assumption is not always true if the input image has more than three bands or is collected by a different sensor other than the PAN. The fusion of MS image with SAR using IHS or BT methods can preserve well the spatial characteristics of the high spatial resolution SAR image, but the fusion product will have spectral distortion which causes colour deformation in the fused product. The colour distortion of IHS

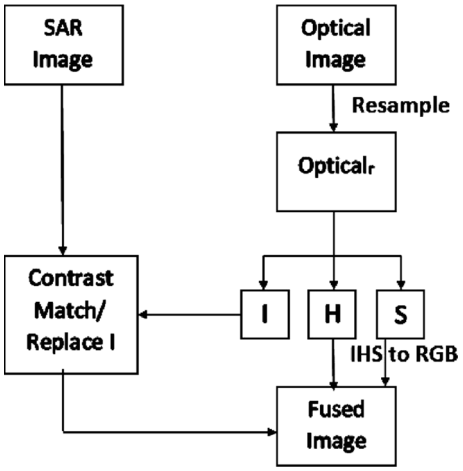

Fig. 2 Schematic of IHS transform

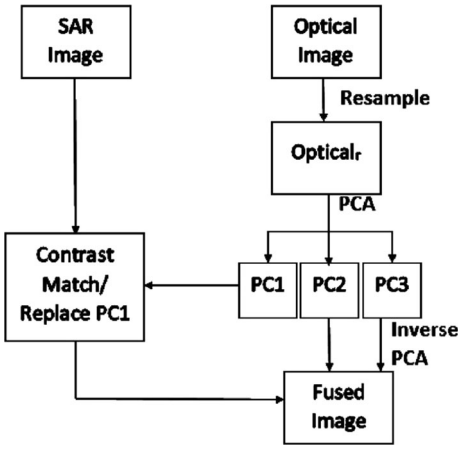

Fig. 3 Schematic of PCA transform

technique is often significant (Srimani and Prasad 2014), and it may not produce good results when fusing SAR imagery with optical imagery (Helmy et al. 2010).

Principal Component Analysis (PCA)

The PCA transform is a statistical technique which converts MS bands that are correlated into uncorrelated components. This method generates a new set of variables, called principal components, and each principal component is a linear combination of the original variables (Kaur and Khullar 2013). Generally, 95% of the total variance is contained in the first three principal components. The first principal component is taken in the direction with the maximum variance so that the first PC band contains the most amount of information of the original image. The first principal component is replaced by the PAN/SAR image. As a final step, inverse PCA transform is performed to obtain new RGB bands of the MS image from principal components. The method is successful in preserving the colour content of the input MS image; however, it produces blocking artefacts (Park and Kang 2004). This problem is getting worse when different sensors are used. The schematic of PCA transform is shown in Fig. 3.

Wavelet-PCA Transform (W-PCA)

The wavelet transform is a mathematical tool which can be applied to fuse images following the concept of the multi-resolution analysis (Mallat 1989; Yunhao et al. 2006). Wavelet-PCA transform method is a combination of traditional PCA method and Wavelet Transform. The schematic of W-PCA transform is shown in Fig. 4. Initially, PCA is applied to the MS image and first principal component (PC1) is obtained. A new SAR image (SAR_{PC1}) whose histogram matches that of the PC1 image has been generated. In the wavelet decomposition, four wavelet coefficients are used for each of PC1 and SAR_{PC1} to generate a half-resolution approximation image with three wavelet coefficient images corresponding to horizontal decomposition (HD), vertical decomposition (VD) and diagonal decomposition (DD) (Yusuf et al. 2013). Then, the coefficients of the SAR image representing the spatial detail information is injected into the PC1 image through the inverse multi-resolution wavelet decomposition. By performing wavelet reconstruction, the new PC1 component is obtained and then the inverse transform is applied on the image to construct a fused RGB image (Srimani and Prasad 2014).

All of the fused images will gain spatial information from the PAN/SAR images. However, the colour effect behaves differently from different methods.

Quality Assessment

Visual Analysis

Quality of the fused images is analysed visually for the performance of fusing techniques. For this purpose, spectral preservation of features in the fused images is compared with that of MS image. Although the visual inspection is easy and direct, it is highly subjective and cannot be used to accurately evaluate the practical effects of the algorithms. Therefore, the performance of each method is further analysed quantitatively, based on two aspects: the spectral quality and the spatial quality. Correlation coefficient (CC), Root Mean Square Error (RMSE), ERGAS index and UIQI have been used for spectral quality assessment. High Pass Correlation Coefficient (HPCC) and entropy have been used for the spatial quality assessment.

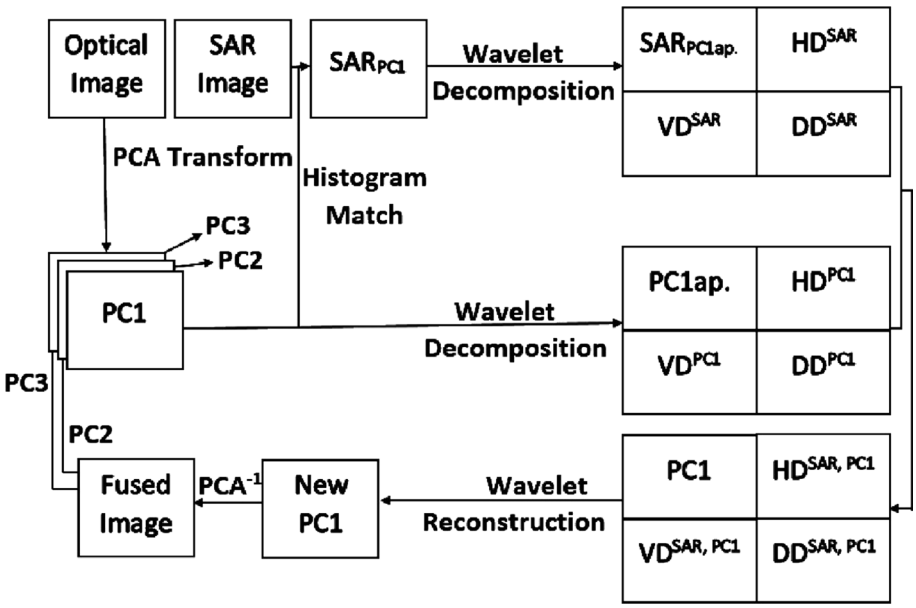

Fig. 4 Schematic of W-PCA transform

Spectral Evaluation

Correlation Coefficient (CC) The correlation coefficient is used to compute the similarity of spectral features between the reference image and fused image (Jagalingam and Hegde 2015). Here, the CC between the original LISS-4 image and the fused image is calculated using Eq. (2).

$$\mathrm{CC}(A,B) = \frac{\sum_{i=1}^{m}\sum_{j=1}^{n}(F(i,j)-\bar{F})(R(i,j)-\bar{R})}{\sqrt{\left(\sum_{i=1}^{m}\sum_{j=1}^{n}(F(i,j)-\bar{F})^2\right)\left(\sum_{i=1}^{m}\sum_{j=1}^{n}(R(i,j)-\bar{R})^2\right)}} \quad (2)$$

where F and R represent DN values of fused and MS images, respectively, $\bar{F}$ and $\bar{R}$ represent the mean of the DN values of fused and MS images, respectively, (i, j) represents pixel index, and m, n represents the size of the image (rows, columns). Higher correlation coefficient between the fused and original MS image indicates better the spectral preservation of the original image in the fused image.

Root Mean Square Error (RMSE) The RMSE is commonly used to compare the difference between the reference image and fused image by directly computing the variation in pixel values (Zoran 2009; Jagalingam and Hegde 2015). It is determined using Eq. (3).

$$\mathrm{RMSE} = \sqrt{\frac{1}{m\times n}\sum_{i=1}^{m}\sum_{j=1}^{n}|R(i,j)-F(i,j)|^2} \quad (3)$$

where F and R represent the DN values of the fused and MS images, respectively, (i, j) represents pixel index, and m, n represents the size of the image. The lower the RMSE value, the better the correspondence between the fused image and the original MS image, the ideal value of RMSE is 0.

Erreur Relative Globale Adimensionnelle de Synthèse (ERGAS) ERGAS is a relative adimensional global error in synthesis and is computed using Eq. (4) (Wald 2002),

$$\mathrm{ERGAS} = 100\times\frac{h}{l}\sqrt{\frac{1}{N}\sum_{k=1}^{N}\frac{(\mathrm{RMSE}(k))^2}{M_k^2}} \quad (4)$$

where h is the spatial resolution of the SAR image, l is the respective resolution of the MS image, N is the number of the bands, and M_k is the mean of the kth band between original MS and fused images. Lower the ERGAS values, the better the spectral quality of the merged images (Sobrino 2002).

Universal Quality Index (UIQI) Instead of using traditional error summation methods, the method proposed by Wang and Bovik (2002) was designed to model any image distortion via a combination of three factors: loss of correlation, luminance distortion, and contrast distortion. The Universal Quality Index (UIQI) is calculated using Eq. (5).

$$\mathrm{UIQI}(x,y) = \frac{\sigma_{xy}}{\sigma_x\sigma_y}\,\frac{2\bar{x}\bar{y}}{\bar{x}^2+\bar{y}^2}\,\frac{2\sigma_x\,\sigma_y}{\sigma_x^2+\sigma_y^2} \quad (5)$$

where x is the original MS image and y is the fused image, $\bar{x}$ is the mean of the original MS image, $\bar{y}$ is the mean of the fused image, n is number of bands in MS image, σ_x^2 is the variance of x, σ_y^2 is the variance of y, and σ_{xy} is the covariance of x, y. These parameters have been calculated using the following equations.

$$\sigma_x^2 = \frac{1}{n-1}\sum_{i=1}^{n}(x_i - \bar{x})^2 \quad (6)$$

$$\sigma_y^2 = \frac{1}{n-1}\sum_{i=1}^{n}(y_i - \bar{y})^2 \quad (7)$$

$$\sigma_{xy} = \frac{1}{n-1}\sum_{i=1}^{n}(x_i - \bar{x})(y_i - \bar{y}) \quad (8)$$

The first component in Eq. (5) measures the degree of linear correlation between and x and y. The second component measures how close the mean luminance is between x and y. The third component measures how similar the contrasts of the images are as σ_x and σ_y. The value of the three components is in the range of 0–1, and thus the final value of the quality metric is normalized between 0 and 1 (Blasch et al. 2008). Value of UIQI close to 1 represents the better image quality.

Spatial Evaluation

Spatial quality enhancement in fused images has been evaluated by using High Pass Correlation Coefficient between the original SAR image with the fused image and by comparing the entropy values of the fused image and SAR image.

High Pass Correlation Coefficient (HPCC) The correlation coefficients between the high-pass-filtered fused image and the high-pass-filtered SAR image are used as an index of the spatial quality (Yakhdani and Azizi 2010). The principle is that the spatial information unique in SAR image is mostly concentrated in the high-frequency domain. The higher correlation between the high-frequency components of fused image and the high-frequency component of SAR image indicates that more spatial information from SAR image has been injected into the fusion result. The following convolution mask has been applied for enhancing high-frequency information (Al-Wassai et al. 2011b; Zhou et al. 1998).

$$\begin{bmatrix} -1 & -1 & -1 \\ -1 & 8 & -1 \\ -1 & -1 & -1 \end{bmatrix}$$

Entropy The entropy in a digital image is a measure of information content in the image. For an image with a large number of pixels, Shannon's entropy (Shannon 2001) is generally used to quantify and evaluate the information content of the image (Leung et al. 2001). Using Shannon's information theory, the entropy of SAR image and the fused image are calculated with help of Eq. (9)

$$E = -\sum_{k=0}^{G-1} P(k)\log_2(P(k)) \quad (9)$$

where G is the total number of grey levels, k is the grey level of an individual pixel, and P is the probability of occurrence of k in the image. The amount of image information is bound to be changed after the image fusion (Pandit and Bhiwani 2015). Increase in entropy value of the fused image signifies an increase in the amount of spatial information compared to original SAR image indication greater the quality of the fusion.

Results and Discussion

The outcome of the different fusion techniques and quality assessment of the different techniques have been discussed in the following sections. The improvements in fused products have been investigated by comparing the fused products with the original MS and SAR images. The fused images have a spatial resolution of 2.25 m. The analysis has been carried out with the whole scene and at different feature levels such as crevasses, melt ponds, freshwater lake, blue ice, and lake ice. The standard false colour composite of the fused images has been prepared.

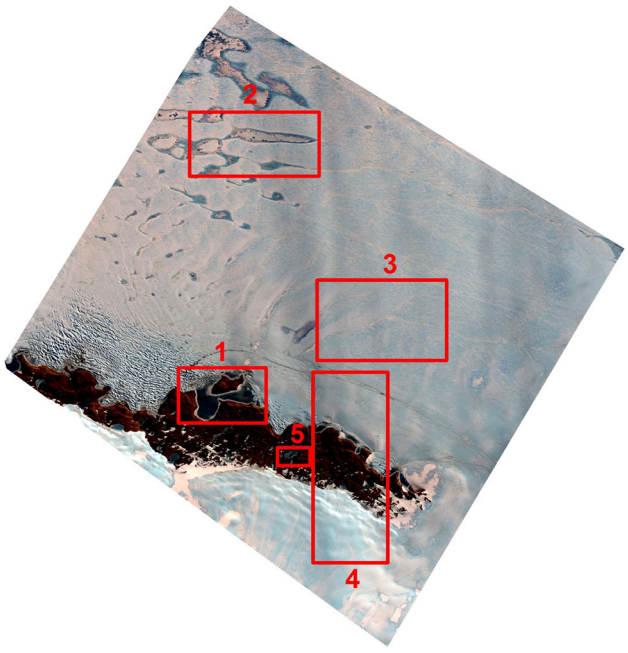

Fig. 5 ResourceSAT-2 LISS-4 image of the study area, marked with major features. 1—Lake Ozhidaniya, 2—melt ponds, 3—crevasses, 4—blue ice, 5—oasis containing lake and lake ice

Visual Analysis

The original ResourceSAT LISS-4 image in which various features are marked is presented in Fig. 5. Figure 6 displays the fused images generated by using different techniques for the whole scene. This figure clearly shows that W-PCA merged product preserves spectral features of MS image and PCA merged product injects more spatial information from SAR image but with a spectral distortion. In order to get more detailed information, feature-wise comparison of merged products with original images for Lake Ozhidaniya, melt ponds, crevasses over ice shelf, blue ice, and oasis containing lake and lake ice has been carried out and the results are presented in Figs. 7, 8, 9, 10, and 11. As seen in Figs. 7, 8, 9, and 10, the meltwater over lake ice, melt ponds, crevasses in ice shelf, and blue ice are better distinguishable in PCA fused images compared to other merged products. As seen in Fig. 7, the melt water in the lake as marked in boxes can be easily discriminated from lake ice in BT, IHS, and PCA fused images, which is not possible in original MS image. In Fig. 8, the small snow covered ice stream connecting between two melt ponds can be easily distinguished in BT, IHS, and PCA fused images compared to original MS image. As shown in Fig. 9, the crevasses marked in boxes are not clearly visible in MS image, but, after fusion using IHS, PCA, and BT techniques, the crevasses are easily detectible. Using MS image as shown in Fg. 10a, it is challenging to discriminate between snow-free ice shelf and blue ice as both these features appear to be blue in colour due to excess loss of air bubbles. But in fused images based on PCA and W-PCA techniques, these features are better distinguishable as seen in Fig. 10e and f. In Fig. 11a, newly formed lake ice which is marked in circle is not identifiable in original MS image, but it is better identifiable in W-PCA fused images. The SAR images are prone to foreshortening, layover, and shadow effect over mountainous regions, and the marked area in rectangle in SAR image (Fig. 11b) shows the foreshortening effect. This effect is visible even after fusion in BT, IHS, and PCA fusion techniques. In general, PCA fusion technique provides better visual enhancement of various ice features compared to other techniques, but

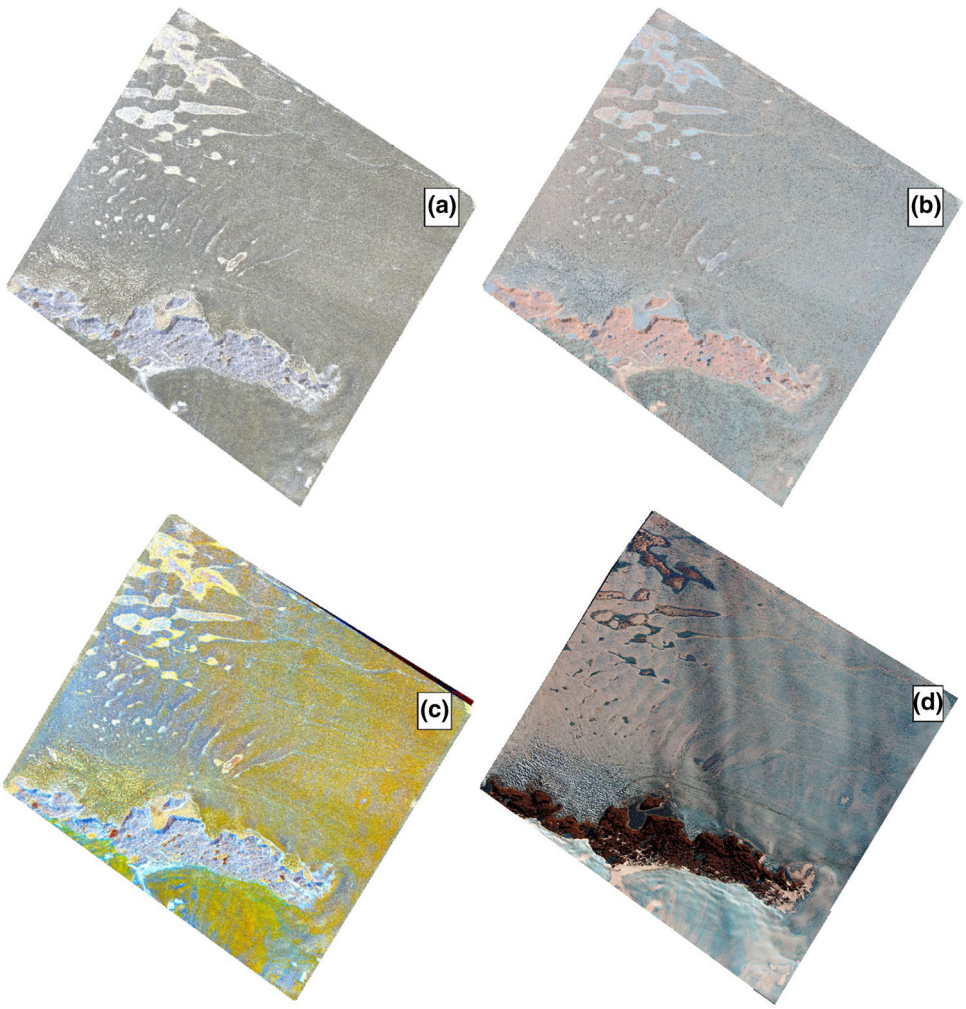

Fig. 6 Merged images of the whole scene. **a** BT, **b** IHS, **c** PCA, **d** W-PCA

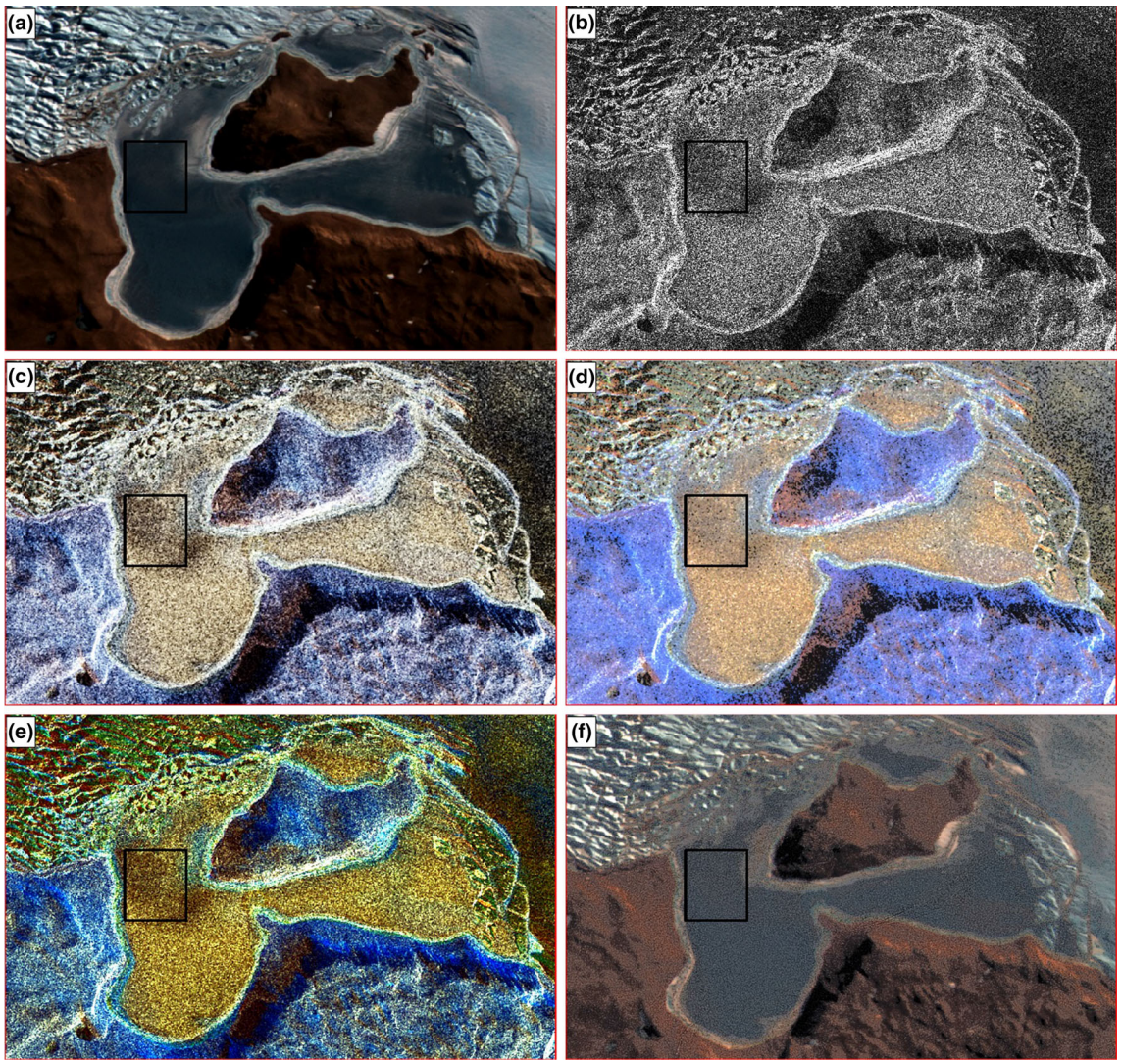

Fig. 7 Original and merged images of ice covered Lake Ozhidaniya near Nadezdhdy Island. **a** LISS-4, **b** SAR FRS-1, **c** BT, **d** IHS, **e** PCA, **f** W-PCA

there is more colour distortion with PCA merging. In general, the spectral characteristics are preserved better in W-PCA fused images and shows poor results in IHS fused images. Similarly, the spatial features in fused images are better enhanced in PCA fused images, but with a colour distortion.

Quantitative Evaluation

The spectral evaluation parameters CC, RMSE, ERGAS, and UIQI averaged for all bands for different ice features based on different fusion techniques are presented in Fig. 12a–d, respectively. For the better preservation of spectral features in fused images, the CC should be close to one, RMSE must be close to zero, ERGAS should be minimum, and UIQI should be close to 1.

Figure 12a clearly reveals that the CC between the multi-spectral images and the fused images with W-PCA technique is highest (more than 0.7) for all features. On the other hand, CC is poorest for BT merged images of all features. The CC values with PCA and W-PCA techniques are found to be high (more than 0.8) for blue ice as well as for melt ponds. The RMSE presented in Fig. 12b shows that values are close to zero for W-PCA and PCA merged images for all features and BT merged product shows very high values for all features. The ERGAS values between MS images and fused images for all features presented in Fig. 12c clearly show values close to zero for W-PCA and PCA merging technique and higher values for BT merged technique for all features. The ERGAS values for IHS technique also indicate lower values except for blue ice. The UIQI values presented in Fig. 12d show high values

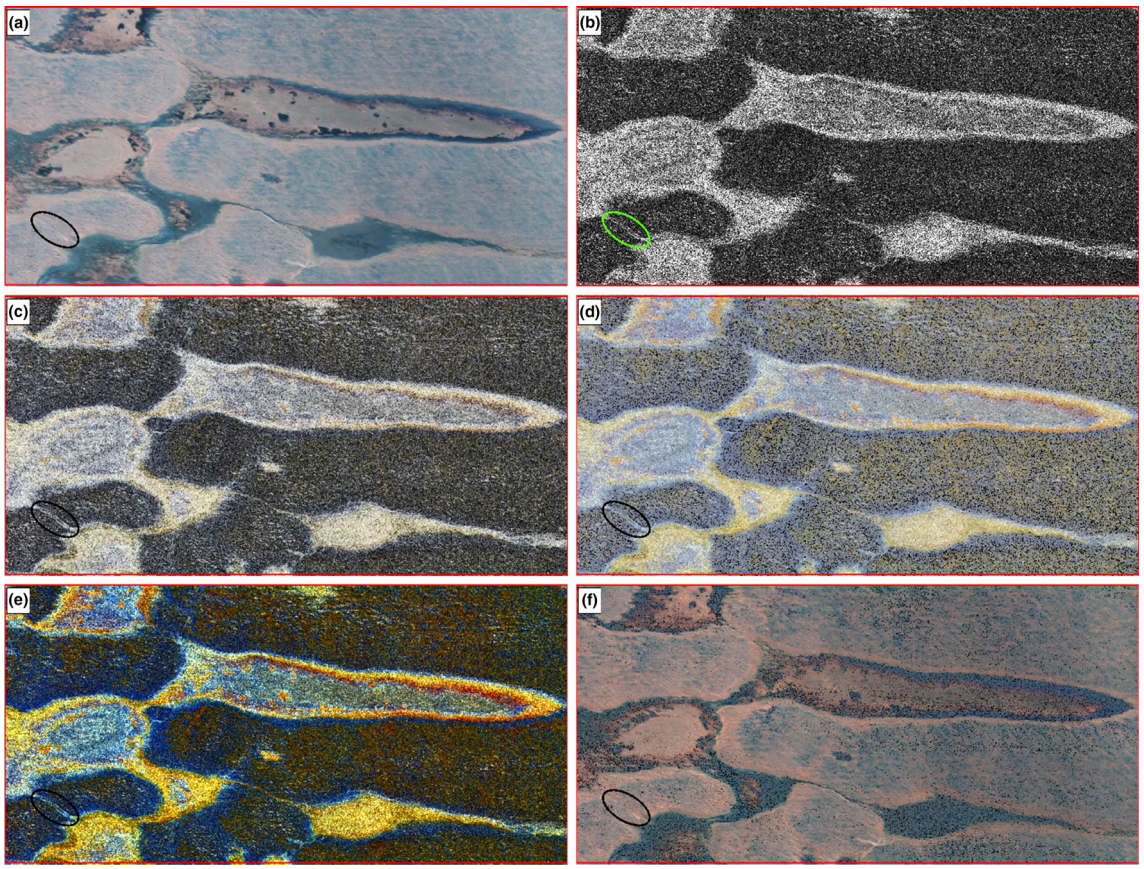

Fig. 8 Original and merged images of melt ponds. **a** LISS-4, **b** SAR FRS-1, **c** BT, **d** IHS, **e** PCA, **f** W-PCA

more of than 0.8 with W-PCA and PCA for all features. Similarly, except for blue ice, IHS technique also shows high values of UIQI. The UIQI values are lower for BT merging technique for all features.

Looking into all four spectral quality parameters, the W-PCA merging technique is the best in preserving the spectral characteristics of MS image in fused images for all features followed by PCA merging technique and followed by IHS. All the four spectral quality parameters of PCA merged product for blue ice and melt ponds support high preservation of spectral features. Except for blue ice, the spectral quality parameters ERGAS and UIQI support good colour preservation for IHS merged products. The BT technique is found to be poorest for all features. From the visual analysis also, it is seen that the colour of the MS image is better preserved in W-PCA fused images. On the other hand, the visual analysis indicates poor colour preservation in PCA merged product.

The spatial evaluation parameter entropy of the SAR image and all the fused images is shown in Fig. 13a, and High Pass Correlation Coefficient (HPCC) between the SAR image and fused images is given in Fig. 13b. Higher values of the entropy of the fused image compared to original SAR image suggest that more spatial information from the SAR image is injected in the fused image. The entropy of the original SAR images is between 4 and 5. The entropy values presented in Fig. 13a show that the highest increase in entropy values compared to the original SAR image is found to be for PCA merged images (> 7) for all the features studied. This suggests that the PCA fused images contain more spatial information in the fused image compared to original SAR image. The increases in entropy values are comparatively higher for oasis containing lake and lake ice in IHS merged image and for lake ice in W-PCA merged images.

The HPCC calculated between high-pass-filtered SAR images and fused images is shown in Fig. 13b. Higher HPCC values indicate that high spatial frequency information from SAR image is efficiently added to the fused image. Generally, higher values of HPCC (around 0.5 or more) are observed for PCA merged products compared to other merged products for all features, suggesting enhancement of spatial features in PCA merged products. For blue ice, the HPCC values are found to be comparatively higher for all merged products except that of BT merged image. The W-PCA merging technique provides significantly higher HPCC for blue ice, but it gives very low values for rest of the features. The HPCC value for

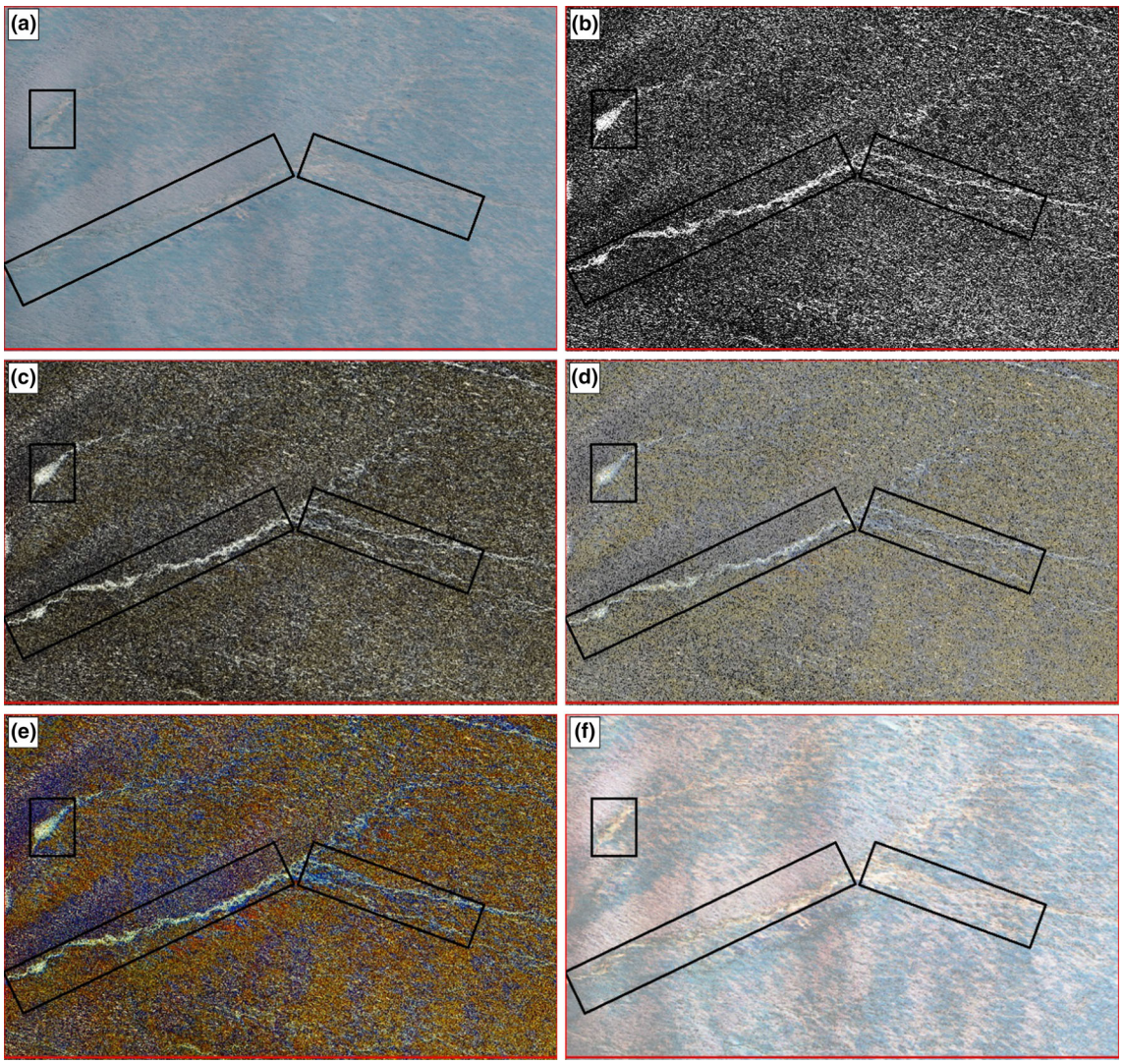

Fig. 9 Original and merged images of part of ice shelf containing crevasses. **a** LISS-4, **b** SAR FRS-1, **c** BT, **d** IHS, **e** PCA, **f** W-PCA

melt ponds is higher in PCA as well as IHS fused images, suggesting that the spatial features of melt ponds are well enhanced by these two fusing techniques. Again, the BT merged products provide poor HPCC values for all the features studied. So, based on both spatial quality parameters, PCA is the best method in injecting surface roughness parameters of SAR into fused images.

The current study area covers features like ice shelf, oasis, fresh water lake, lake ice, melt ponds, crevasses, and blue ice. Blue ice is difficult to distinguish from snow-free ice shelf in SAR image as well as in MS image. But, fusing these two images with PCA and W-PCA techniques helps in better identification of blue ice. The crevasses over ice shelf are clearly distinguishable in the PCA merged product followed by IHS merged products. All the six quality assessment parameters suggest that the melt ponds features are highly enhanced in PCA fused product. Five of the six quality parameters suggest that lake ice features are better enhanced with PCA merged product followed by W-PCA merged product. There are only limited features in the present study area, but using images with extended coverage, we can definitely obtain better results for identification of ice and snow features. In spite of having high-resolution, single-polarization SAR image is not able to identify clearly different ice features.

Conclusion

An attempt has been carried out to fuse RISAT-1 SAR FRS-1 image with ResourceSAT LISS-4 MS images over Indian research station Maitri and surrounding areas for better discrimination of Antarctic ice features. Even though there are a variety of fusion techniques available, the

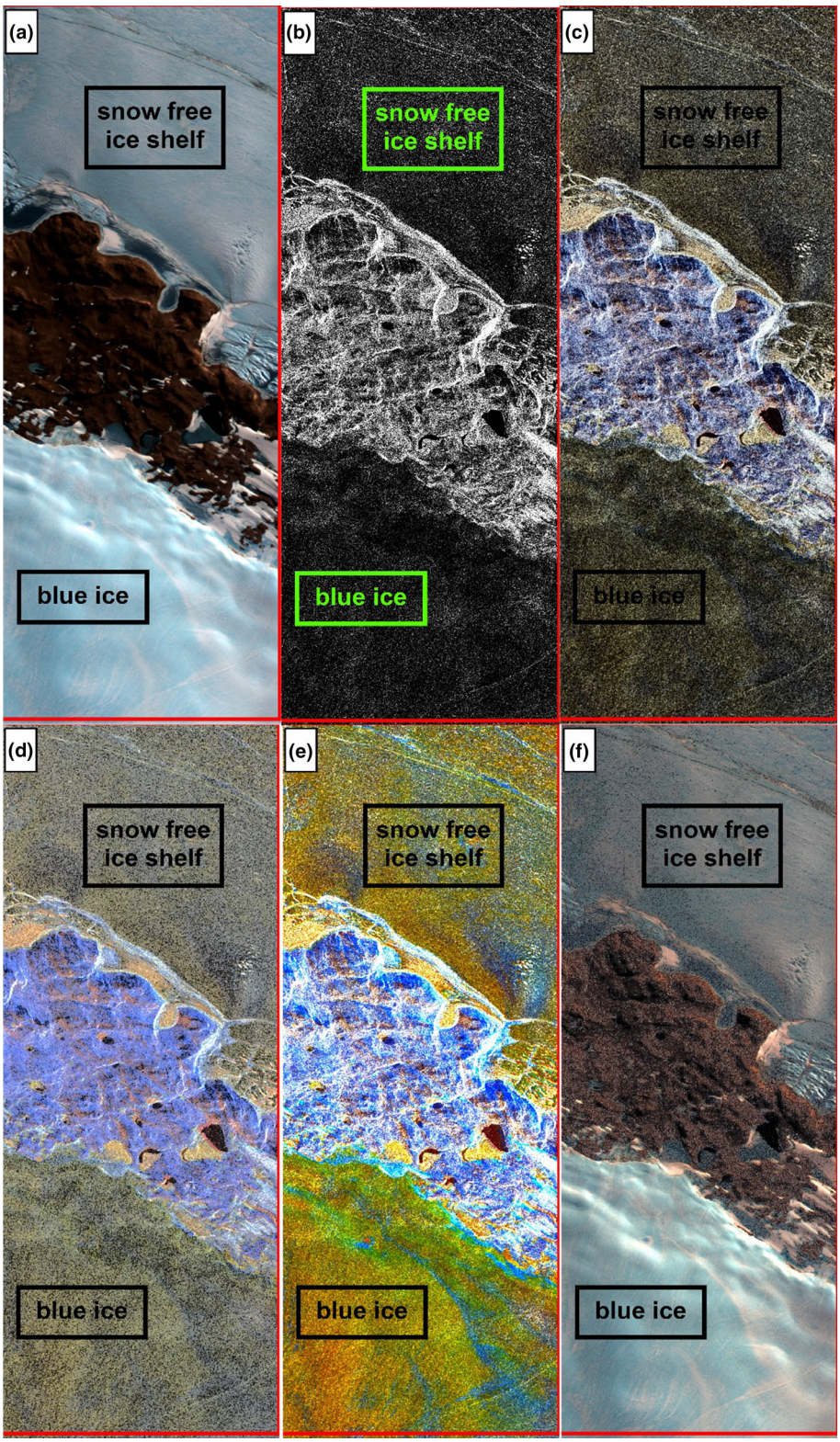

Fig. 10 Original and merged images showing snow-free ice shelf and blue ice. **a** LISS-4, **b** SAR FRS-1, **c** BT, **d** IHS, **e** PCA, **f** W-PCA

standard fusion techniques such as Brovey Transform (BT), Intensity Hue Saturation (IHS), Principal Component Analysis (PCA) and Wavelet-PCA Transform (W-PCA) have been attempted with help of ERDAS IMAGINE software. Comparison of fused images with original SAR and LISS-4 images gives the idea about the success of fusion algorithms and their impacts in extracting the Antarctic ice features. The success of fusion has been

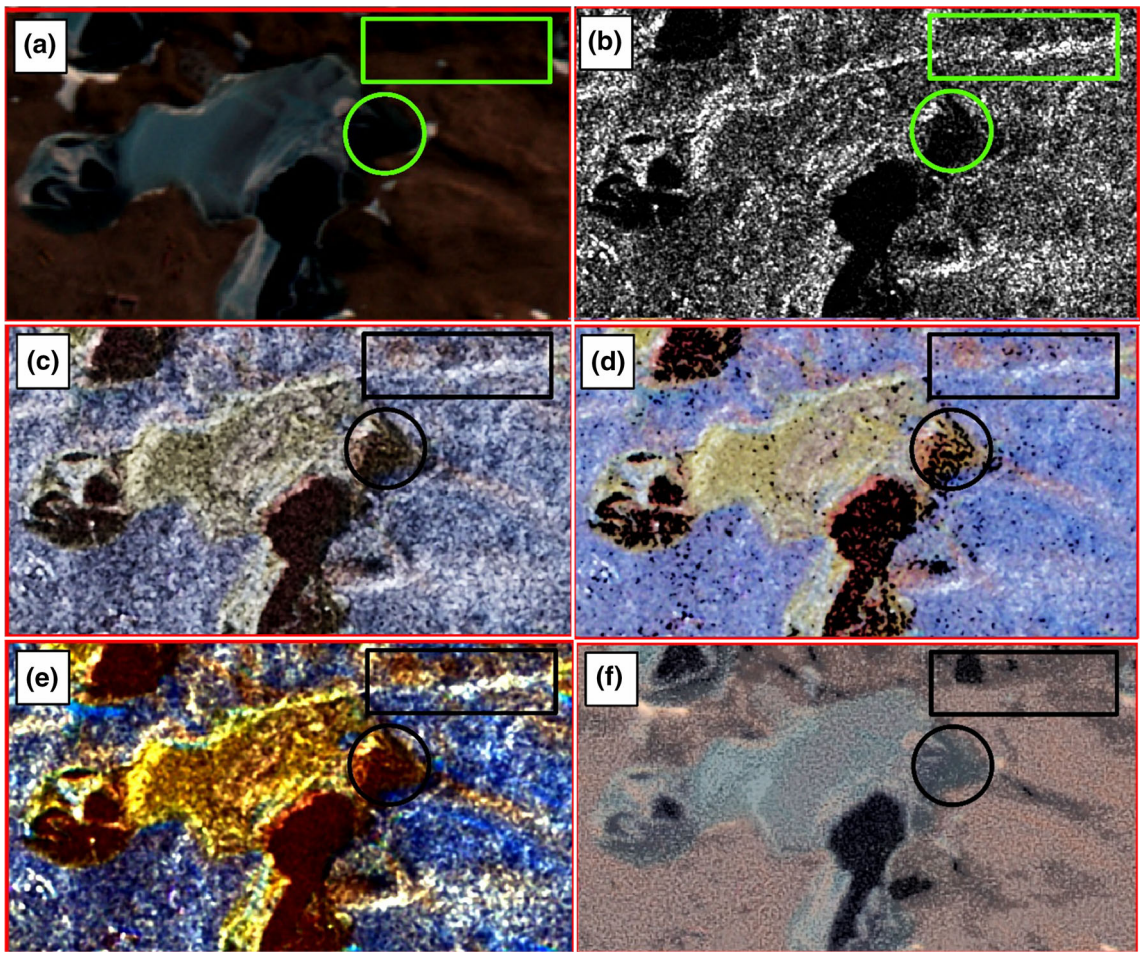

Fig. 11 Original and merged images of oasis containing lake and lake ice. **a** LISS-4, **b** SAR FRS-1, **c** BT, **d** IHS, **e** PCA, **f** W-PCA

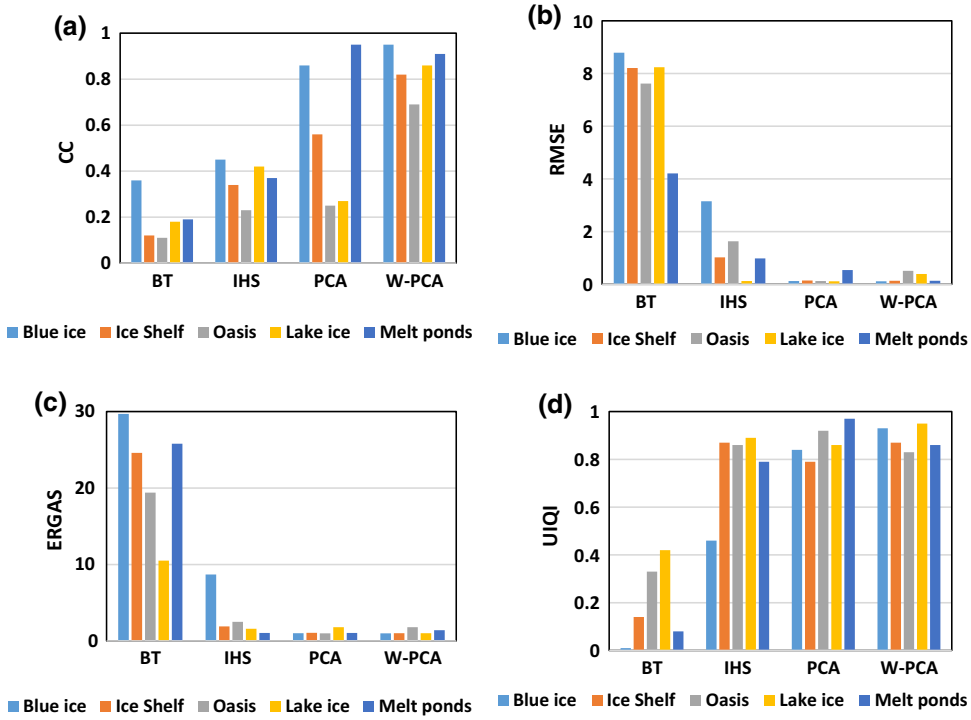

Fig. 12 Spectral evaluation parameters between LISS-4 and fused images for different features. **a** CC, **b** RMSE, **c** ERGAS, **d** UIQI

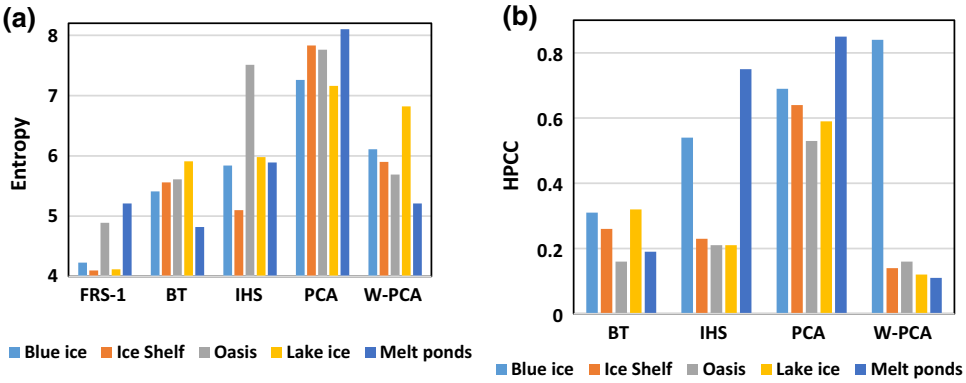

Fig. 13 Spatial evaluation parameters between SAR and fused images. **a** Entropy, **b** HPCC

tested visually and by quantitative methods. For quantitative analysis, both spectral parameters such CC, RMSE, ERGAS and UIQI and spatial parameters such as Entropy and HPCC have been utilized. Certain features are found to be enhanced clearly in some merging techniques while certain techniques are found to be poor for all features. W-PCA fused images of all features show high performance in all spectral quality parameters, clearly indicating that the W-PCA fusion technique enhances the spectral characteristics of LISS-4 MS images in fused images, which is again supported by visual analysis. Among the four algorithms, the W-PCA preserves spectral features MS image in the fused image better than other methods. The PCA fusion also provides ERGAS close to zero, UIQI close to one, comparatively low RMSE, and comparatively high CC. The PCA fusion technique follows the W-PCA techniques in terms of discriminating power, and BT is found to be the poorest technique. Even though there are certain colour distortions with PCA fusion images, the spatial quality evaluation parameters entropy and HPCC show high values for all features in general, suggesting the PCA merging technique retains all spatial variations of SAR in the merged product. Overall, the identification of features such as lake ice, crevasses, blue ice, and melt ponds have been improved with fused images compared to the original MS and SAR images.

With the availability of good temporal resolution datasets, feature extraction over Antarctica can be improved using the merging techniques. The results of the present study can be stabilized by analysing more images of exactly same period. Identification of other Antarctic ice features could be looked into using other fusion techniques. Further studies shall be carried out using classification of fused products to extract Antarctic ice features.

Acknowledgements Authors are thankful to SAC, ISRO, for providing research grant under MOP-III program. Authors acknowledge DST and UGC for the financial assistance extended to the Physics Department, Gujarat University, under FIST and SAP. They are thankful to Dr. Raj Kumar, Deputy Director, EPSA, for his support and the keen interest in this study. The guidance provided by Smt. Arundhati Misra, GD, AMHTDG, and Deepak Putrevu, Head, MTDD, AMHTDG, is greatly acknowledged. Authors sincerely thank the anonymous reviewers and editors for their valuable suggestions and comments.

References

Al-Wassai, F. A., Kalyankar, N. V., & Al-Zaky, A. A. (2011a). Studying satellite image quality based on the fusion techniques. *International Journal of Advanced Research in Computer Science, 2*(5), 354–362.

Al-Wassai, F. A., Kalyankar, N. V., & Al-Zuky, A. A. (2011b). The IHS transformations based image fusion. *Journal of Global Research in Computer Science, 2*(5), 70–77.

Atta, H. A. M. (2012). Different resolution merging methods for environmental areas extraction. *Journal of Engineering, 18*(12), 1335–1343.

Blasch, E., Li, X., Chen, G. & Li, W. (2008). Image quality assessment for performance evaluation of image fusion. In *The proceedings of 11th international conference on information fusion* (pp. 1–6). IEEE.

Chibani, Y. (2007). Integration of panchromatic and SAR features into multispectral SPOT images using the 'a tròus' wavelet decomposition. *International Journal of Remote Sensing, 28*(10), 2295–2307.

Ehlers, M., Klonus, S., Johan Åstrand, P., & Rosso, P. (2010). Multi-sensor image fusion for pansharpening in remote sensing. *International Journal of Image and Data Fusion, 1*(1), 25–45.

Erener, A. & Sebnem, D. (2012). Urban feature detection by using TerraSar-X and optic image. In *International conference on earth science and remote sensing, lecture notes in information technology*, Vol. 30 (pp. 316–321).

Gharbia, R., Azar, A. T., Baz, A. E., & Hassanien, A. E. (2014). Image fusion techniques in remote sensing. ArXiv preprint arXiv:1403.5473.

Helmy, A. K., Nasr, A. H., & El-Taweel, G. S. (2010). Assessment and evaluation of different data fusion techniques. *International Journal of Computers, 4*(4), 107–115.

Jagalingam, P., & Hegde, A. V. (2015). A review of quality metrics for fused image. *Aquatic Procedia, 4,* 133–142.

Jain, S. (2007). Use of IKONOS satellite data to identify informal settlements in Dehradun, India. *International Journal of Remote Sensing, 28*(15), 3227–3233.

Jawak, S. D., & Luis, A. J. (2013). A comprehensive evaluation of PAN-sharpening algorithms coupled with resampling methods for image synthesis of very high resolution remotely sensed satellite data. *Advances in Remote Sensing, 2*(04), 332–344.

Karhe, R. R., & Chandratre, Y. V. (2016). RADAR image fusion using wavelet transform. *International Journal of Advanced Engineering, Management and Science, 2*(3), 4–13.

Kaur, A., & Khullar, S. (2013). Image fusion using IHS, PCA and wavelet technique. *International Journal of Computer Science and Communication Engineering, 2*(2), 92–94.

Lee, J. S. (1981). Speckle analysis and smoothing of synthetic aperture radar images. *Computer Graphics and Image Processing, 17*(1), 24–32.

Leung, L. W., King, B., & Vohora, V. (2001). Comparison of image data fusion techniques using entropy and INI. In *22nd Asian conference on remote sensing*, Vol. 5 (pp. 9–14).

Mallat, S. G. (1989). A theory for multiresolution signal decomposition: The wavelet representation. *IEEE Transactions on Pattern Analysis and Machine Intelligence, 11*(7), 674–693.

Mandhare, R. A., Upadhyay, P., & Gupta, S. (2013). Pixel-level image fusion using brovey transforme and wavelet transform. *International Journal of Advanced Research in Electrical, Electronics and Instrumentation Engineering, 2*(6), 2690–2695.

Misra, I., Gambhir, R. K., Moorthi, S. M., Dhar, D., & Ramakrishnan, R. (2012). An efficient algorithm for automatic fusion of RISAT-1 SAR data and ResourceSAT-2 optical images. In *4th International conference on Intelligent Human Computer Interaction (IHCI)* (pp. 1–6). IEEE.

Misra, T., Rana, S. S., Desai, N. M., Dave, D. B., Rajeevjyoti, Arora, R. K., et al. (2013). Synthetic aperture radar payload on-board RISAT-1: Configuration, technology and performance. *Current Science, 104*(4), 446–461.

Pal, S. K., Majumdar, T. J., & Bhattacharya, A. K. (2007). ERS-2 SAR and IRS-1C LISS III data fusion: A PCA approach to improve remote sensing based geological interpretation. *ISPRS Journal of Photogrammetry and Remote Sensing, 61*(5), 281–297.

Pandit, V. R., & Bhiwani, R. J. (2015). Image fusion in remote sensing applications: A review. *International Journal of Computer Applications, 120*(10), 22–32.

Park, J. H., & Kang, M. G. (2004). Spatially adaptive multi-resolution multispectral image fusion. *International Journal of Remote Sensing*, *25*(23), 5491–5508.

Rahman, M. M., Tetuko Sri Sumantyo, J., & Sadek, M. F. (2010). Microwave and optical image fusion for surface and sub-surface feature mapping in Eastern Sahara. *International Journal of Remote Sensing, 31*(20), 5465–5480.

Ramadan, T. M., Nasr, A. H., & Mahmood, A. (2006). Integration of Radarsat-1 and Landsat TM images for mineral exploration in East Oweinat district, south western desert, Egypt. In *ISPRS commission VII mid-term symposium remote sensing: From pixels to processes* (pp. 244–249). Enschede.

Ricchetti, E. (2001). Visible infrared and radar imagery fusion for geological application: A new approach using DEM and sun-illumination model. *International Journal of Remote Sensing, 22*(11), 2219–2230.

Schmitt, M., Tupin, F., & Zhu, X. X. (2017). Fusion of SAR and optical remote sensing data: Challenges and recent trends. In *IEEE International Geoscience and Remote Sensing Symposium (IGARSS)* (pp. 5458–5461).

Shannon, C. E. (2001). A mathematical theory of communication (Parts I and II). *Bell System Technique Journal, 27,* 379–423.

Sobrino, J. A. (Ed.). (2002). *Recent advances in quantitative remote sensing* (p. 984). Valencia: Universitat de València.

Srimani, P. K., & Prasad, N. (2014). Analysis and comparative study of image fusion techniques for land use and land cover classification on Anthrasanthe Hobli, Karnataka: Case study. *International Journal of Engineering Research and Technology, 3*(6), 1703–1711.

Wald, L. (2002). *Data fusion: Definitions and architectures: Fusion of images of different spatial resolutions* (p. 197). Paris: Presses des MINES.

Wang, Z., & Bovik, A. C. (2002). A universal image quality index. *IEEE Signal Processing Letters, 9*(3), 81–84.

Yakhdani, M. F., & Azizi, A (2010). Quality assessment of image fusion techniques for multi sensor high resolution satellite images. In *Proceedings of ISPRS TC VII symposium-100 years ISPRS XXXVIII*, Part 7B (pp. 201–209).

Yunhao, C., Lei, D., Jing, L., Xiaobing, L., & Peijun, S. (2006). A new wavelet-based image fusion method for remotely sensed data. *International Journal of Remote Sensing, 27*(7), 1465–1476.

Yusuf, Y., Sri Sumantyo, J. T., & Kuze, H. (2013). Spectral information analysis of image fusion data for remote sensing applications. *Geocarto International, 28*(4), 291–310.

Zhou, J., Civco, D. L., & Silander, J. A. (1998). A wavelet transform method to merge Landsat TM and SPOT panchromatic data. *International Journal of Remote Sensing, 19*(4), 743–757.

Zoran, L. F. (2009). Quality evaluation of multiresolution remote sensing images fusion. *UPB Scientific Bulletin Series C, 71*(3), 38–52.